Research Article Vol. 1, No. 4 / 15 Apr 2022 / Optics Continuum 759
OPTICS CONTINUUM

Time-resolved holographic study of laser-induced fatigue in bulk of sapphire and fused silica

BALYS MOMGAUDIS,* MIKAS VENGRIS, AND ANDRIUS MELNINKAITIS

Vilnius University, Laser research center, Saulėtekio al. 10, Vilnius, Lithuania
*balys.momgaudis@ff.vu.lt

Abstract: In this work, the fatigue effect caused by multi-pulse laser irradiation in bulk of transparent optical medium for ultrashort pulses is investigated. Time-resolved digital holography is used as a sensitive tool for quantifying changes in material response below single-shot damage threshold. In case of two investigated fused quartz samples the survivable dose is limited by increase in the yield of free electrons and self-trapped exciton densities with number of expositions prior to damage formation. Meanwhile, no change was detected in free electron plasma for sapphire before multi-pulse damage which lead to nondeterministic damage. It was estimated that optical damage could form bellow critical plasma density for all samples. The data on low energy irradiation and damage morphology suggest a strong contribution from defects to the initiation of multi-pulse optical damage in bulk media.

1. Introduction

The degradation of optical components is an important problem in laser technology. The growing capabilities of modern lasers impose ever-more stringent requirements on the optics that have to withstand the light of extreme parameters: ultrashort pulses, octave-spanning spectra, terawatt and higher intensities. The limiting values of these parameters are often attempted to capture using a single number, namely the optical damage threshold. However, the physics of optical damage turns out to be much more complex than staying away from a clear-cut fluence limit. One interesting effect is that with the increase in intensity the number of pulses necessary to trigger multi-pulse damage decreases [1] and the material properties were shown to change faster [2]. In the worst case scenario, even slight degradation of optical components may lead to feedback loops resulting in catastrophic damage. This is so called optical fatigue effect. Damage tends to propagate between the elements driven by diffraction and filamentation therefore even a single damaged element could cause a collapse of the entire optical powertrain. This means that complex systems necessary to produce extreme parameters of light are also the most susceptible to the fatigue effect due to strain on components and their variety. To protect such expensive systems from failure, it is important to asses not only laser-induced damage threshold but also fatigue of optical materials that limits the overall service life time of the components and to understand the mechanisms driving this phenomenon.

Single shot optical damage has been investigated in detail, however there is still no full picture for the multi-shot case. Fatigue related phenomena were first observed in mid-eighties and extensive studies have been made into the subject with long duration pulses (>1ns). Two main mechanisms are thought to be responsible for fatigue in wide bandgap glasses depending on the wavelength of light being used. At longer wavelengths, where the energy of a photon ($\hbar\nu$) is less then the half of the bandgap(E_g) of the material ($\hbar\nu<E_g/2$), the light degrades the glass network forming bonds (Si-O-Si in silica glasses) and reduces the intensity threshold the material can withstand. The correlation between the concentration of bonds and optical damage threshold were confirmed experimentally [3]. Meanwhile, higher energy photons ($\hbar\nu>E_g/2$)

#453503 https://doi.org/10.1364/OPTCON.453503
Journal © 2022 Received 10 Jan 2022; revised 17 Mar 2022; accepted 23 Mar 2022; published 1 Apr 2022

OPTICS CONTINUUM

were responsible for the creation of localised colour centers. These in turn increase the refractive index and promote self-focusing leading to a feedback loop that culminates in damage caused by accumulation of mechanical stress. This phenomenon was observed in both large band gap glasses and crystals [4,5]. However, most studies were done with relatively long duration laser pulses that were commonly available at the time. Unreliable performance of devices producing shorter light pulses of the time lead to a belief that the cause of multi-pulse damage can be attributed to inhomogenities of the material or fluctuations in pulse parameters. [6–9].

The development of modern femtosecond laser sources featuring increased stability together with ongoing research in optical damage threshold were able to confirm the degradation in optical damage threshold with increasing number of sub-picosecond pulse expositions [10–15]. However, very few studies have investigated the principles governing the phenomenon for ultrashort pulses in bulk media, while it is known that the physical properties differ between bulk and surface. [16,17] On one hand investigations into the intrinsic damage in bulk silica lead to the conclusion that the intrinsic threshold value is the same between single-shot and multi-shot damage [18]. On the other hand without sufficiently tight focusing conditions to achieve intrinsic damage fused quartz has been shown to change it's properties depending on the number of interactions [2]. This same response is the basis for the most prevalent idea in the field that optical fatigue caused by femtosecond pulses is due to a positive feedback loop involving generation of self-trapped excitons (STE) and colour centers [13]. In this loop, the light pulse generates free electron plasma, which relaxes into STE and a fraction of these form colour centers (deep level traps). The traps with long lifetimes enhance the absorption leading to an increase in the density of free electron plasma thus forming the feedback. Plasma density reaching a critical point is a commonly used criterion for optical damage [19] also used in this model. It is important to note that this fatigue model was developed for fused quartz and does not easily extend to other materials. To address this issue, a more phenomenological model was proposed for wider application [20]. However, such approach does not leave any room for accounting of common physical processes between different materials. Therefore, the goal of the study is to investigate the mechanisms underlying the fatigue of optical damage threshold in bulk media of different materials, identification of contributing factors and how it can be interpreted in the framework of the current theory.

Achieving these goals requires direct observation of the phenomenon as well as selection of suitable time frames to map the transient material response to multiple excitation events. We employ time-resolved digital holography (TRDH) to observe and measure the interaction of light and the material at different time frames, how it changes with increasing number of applied laser pulses, different energy levels and materials. Such collection of quantitative data is a necessary step towards understanding the laser fatigue in bulk materials and in general. Furthermore, it can be used to determine the numerical values of otherwise free parameters governing the current models of optical fatigue.

2. Materials and methods

Pump-probe off-axis time-resolved digital holography [21] was the main tool employed in the study. The principal architecture of the system can be seen in Fig. 1. The pulses were characterised using second harmonic scanning autocorrelator "Geco" designed by "Light Conversion". The fundamental radiation of Yb:KGW laser at 1030 nm central wavelength is used as the pump with duration 360 fs at full width half maximum (FWHM). The probe is obtained by using a single-pass noncollinear optical parametric generator. A seed of supercontinuum radiation is amplified by 343 nm light within BBO crystal to create a pulse with central wavelength of 550 nm that is further compressed down to 35 fs (FWHM).

The excitation is achieved by sharp focusing of the pump beam within the bulk sample using 0.18 NA aspherical lens. The time dependence of laser induced changes in the optical properties of the sample are investigated by changing delay of the probe pulse with respect to pump pulse.

OPTICS CONTINUUM

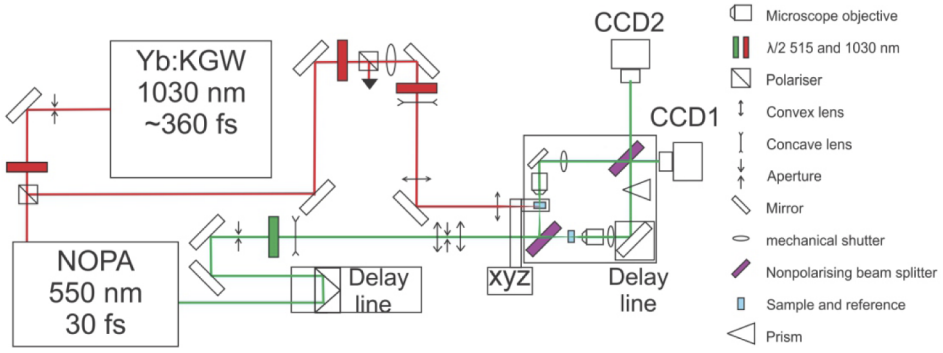

Fig. 1. The principle optical scheme of pump-probe time-resolved digital holography microscopy setup.

This is achieved by translating the retroreflector attached to a mechanical delay line within probe branch.

Using time-resolved digital holographic approach both amplitude and phase changes of light transmitted trough laser excited zone of the sample can be measured. The recording of a digital hologram is realized using a Mach-Zehnder interferometer. The probe light is first expanded to fill a 25 mm diameter lens with a focal distance of 75 mm and then focused past the first non-polarising beamsplitter resulting in focal spots in each of the interferometer arms. The light in the object branch passes trough the excited volume of the sample which is imaged via 20x 0.4 NA infinity-corrected microscope objective and 200 mm focusing lens onto CCD2. This light is split by the second beamsplitter before it passes through the imaging lens and a fraction of it reaches CCD1. Here it interferes with the light from the reference branch which is reflected by the same beamsplitter. By interfering object and reference beams the information on both amplitude and phase of the distortion is recorded on CCD1. To minimize the optical path and dispersion difference, sample of same material and size as well as microscope objective is placed in the reference branch. In order to obtain the wide field of interference in off-axis holography setup with short pulses, it is necessary to tilt the pulse front to match the angle of intersection of the two beams. The tilted front pulse is achieved by using a 30° fused quartz prism in the reference branch. The recorded hologram is used to numerically reconstruct the phase and amplitude as it is seen on CCD1. In this way 20 mrad phase noise (at the level of two standard deviations) in a single-shot experiment was achieved. This error can be further reduced by averaging of the digital holograms. The system was also able to resolve lines of USDF 1951 target less then 2 um in diameter while the temporal resolution of 35 fs was limited by the duration of the probe pulse.

In real world applications, it may take months or more to observe the phenomenon of optical fatigue depending on the repetition rate, intensity of light, workload of the equipment and similar factors. However, this is unfeasible in laboratory setting. Therefore, the minimal energy that is capable of producing optical damage within a number of pulses achievable on the time scale of tens of minutes was chosen as a proxy to mimic multi-pulse fatigue phenomenon. In this case the highest practical number of pulses was 2500. The suitable energy intervals for each sample were found using transmission images while changing the energy of the pump pulse and monitoring the affected volume.

In order to optimise the observation of material response to multiple shots the following measurement algorithm was devised. Due to the limited acquisition rate of the cameras the frequency of the laser was set to 20 Hz using a pulse picker. Every second shot was recorded on the cameras. Before starting the exposure sequence, a hologram of undisturbed sample was recorded and used as a reference in subsequent steps. Next, the desired pulse energy and time

OPTICS CONTINUUM

delay are set. The acquisition of excitation holograms starts when the mechanical pump shutter is opened. A desired number of photos are obtained and averaged into the final digital hologram. Using numerical reconstruction algorithm described in Ref. [22], the numerical values of phase and amplitude maps are calculated for the given number of expositions. The pump shutter is then closed shut and a new intermediate hologram is recorded to be used as the new reference. The cycle continues until optical damage is observed. At that point the sample is moved to a new position and a experimental sequence starts a new.

The experimental conditions are summarised in the Table 1. The duration of the pulses were measured using a second harmonic autocorrelator (Geco, Light Conversion) while prechirping the probe pulse to account for the sample dispersion as the volume excited by the pump is several hundred micrometers from the exit surface for the probe. To avoid the interference from sample edge, the position of the excitation volume was set to $500 \pm 50\mu$ m behind the entry surface of the pump pulse. The diameter of the pump was measured using imaging microscope with NA 0.4 and tube lens resulting in 19.2x magnification and a CCD camera. It was later used to evaluate the radius by fitting a two dimensional Gaussian profile. Two UVFS samples were chosen due to how well known the material is and how commonly it is used for transmission optics. These two samples are both from the same supplier (Altechna, Lithuania) and are produced by the same manufacturer(Corning 7980 0F). The main difference is time of acquisition indicating different batches. UVFS1 was obtained in the year 2013 meanwhile UVFS2 was obtained in the year 2020. To illustrate differences and similarities sapphire was chosen as a crystalline counterpart to the amorphous fused quartz. Sapphire sample was received from a different supplier (Eksma Optics, Lithuania) in 2021. The orientation of sapphire lattice is such that the optical axis perpendicular to both pump and probe pulses and parallel to the direction of polarization.

Table 1. Summary of exact experimental conditions.

Material	Dimensions	t_{FWHM}, pump	$w_{e^{-2}}$, pump	t_{FWHM}, probe
UVFS1	$4x10x20mm$	$352fs$	$2.84\mu m$	$55fs$
UVFS2	$5x20x40mm$	$360fs$	$2.85\mu m$	$37fs$
Sapphire	$2x5x20mm$	$375fs$	$2.83\mu m$	$36fs$

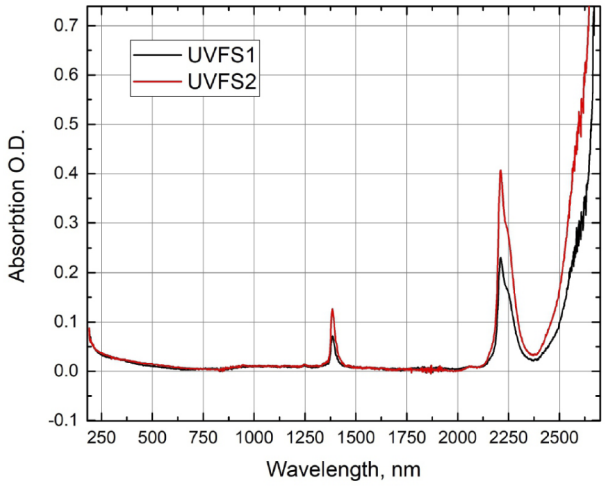

Fig. 2. The comparison between the absorption spectra of UVFS1 and UVFS2 samples.

OPTICS CONTINUUM

To see if there are any fundamental differences between the fused quartz samples and their purity the absorption spectra in the range of 190-3000 nm was measured. The obtained spectra in the range 190-2400 nm is shown in Fig. 2 (their differences will be further discussed below).

3. Experiment results

The first step was to measure the response of material during the excitation and to see if there are any significant changes in material response prior to damage. For fatigue studies the optimal time delay choice was necessary. Therefore the temporal evolution of light and material interaction for each sample was done. The phase maps for UVFS2 depicting the material response at different delay times are shown in Fig. 3. All the pictures in this work illustrating the zone of interest are oriented so that the direction of pulse propagation is up.

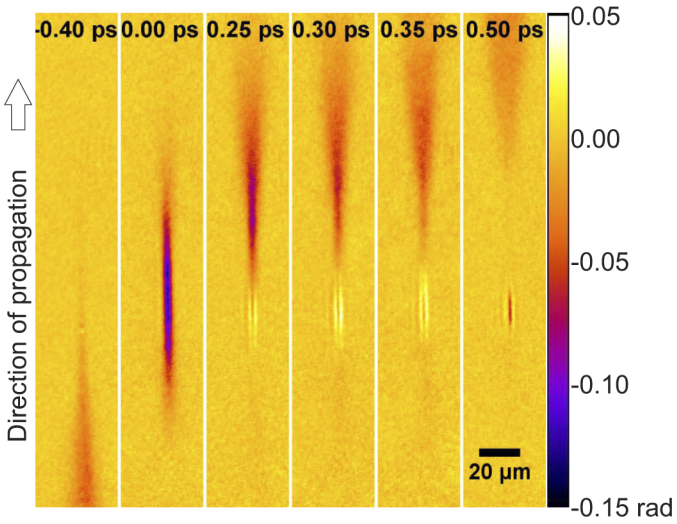

Fig. 3. The spatial material response in radians to low intensity ($0.46\mu J$) pump pulse in UVFS2 sample at different time delays. Initial negative phase shift - optical Kerr effect is followed by free electron plasma (localised positive phase shift) and STE (localised negative phase shift).

The sequence begins with the propagation of light that results in the increase of refractive index due to optical Kerr effect. Observed as a negative phase shift. When the irradiation reaches the close proximity of focal point, the nonlinear absorption and avalanche ionization starts. This results in creation of free electron plasma. The electron plasma decreases the refractive index and therefore it is visible as positive phase change. This plasma has a short life time of 170 fs [23] in fused quartz due to inherent relaxation via STE. The excitons can create both positive or negative refractive index changes depending on the probe wavelength but in this experiment they exhibit the increase in refractive index and therefore can also be observed as negative phase shift.

The primary interest of the study lies in the change of the material response as a function on the number of pulses received prior to optical damage. Multiple delay times were investigated. The first one - zero delay - indicating the moment of maximum overlap between optical Kerr effect and the area of focal spot. In this time frame, there is no observable changes in the response to increasing number of pulses indicating that no significant material modification takes place in the volume prior to focal point before optical breakdown. This suggests that there is no change in focusing conditions and it should not play a role in optical damage formation. The other two time frames were determined by the maximum observable free electron plasma and self-trapped

OPTICS CONTINUUM

exciton signal values at low incident energy pulses in fused quartz samples. The response of free electron plasma is investigated at the time delay of 300 fs and excitons at that of 1100 fs for both UVFS samples. It must be noted that these values are only applicable to low energy pump pulses because at higher energies it is limited by increased temporal overlap between the three contributing phenomena. In sapphire, self-trapped excitons are not observed using digital holography. The life time of plasma is long in comparison to fused quartz, and temporal overlap with Kerr effect can be easily avoided. Due to negligible relaxation, the response of free electron plasma at 2 ps delay time was investigated.

The next step was to observe optical damage due to fatigue. Transmission images of damage were obtained by subtracting the initial transmission photo (unexposed sample) from the photo of damage taken several seconds after the excitation by the laser pulse. Typical photos indicating the damage morphology for each material are shown in Fig. 4. The dimensionless number on the bottom left of the photo indicates the accumulated pulses in the site when the photo is taken. The accumulated pulses in subsequent pictures are indicated in a similar fashion. It can be seen that for all the investigated materials the damage initiates as a small dot with the dimensions smaller then the resolution limit of the system imaged as as a blurred circle of reduced transmission indicated by darker colour in transmission photos. It then grows in size and intensity with increase in number of applied pulses. Interestingly enough, at higher pump energy less pulses are needed to trigger apparent damage and for UVFS2 the damage morphology changes. It starts as refractive index modification, observed as a darker cylinder in the fourth panel. While, this effect appears as absorption, the light is actually refracted to the sides which can be verified by integrating the change in transmission over the field of view. Due to redistribution of light, the integral of transmission is equal to one. It was also observed that subsequent pulses will fragment the modification seen in UVFS2 into multiple damage points as seen in the last picture.

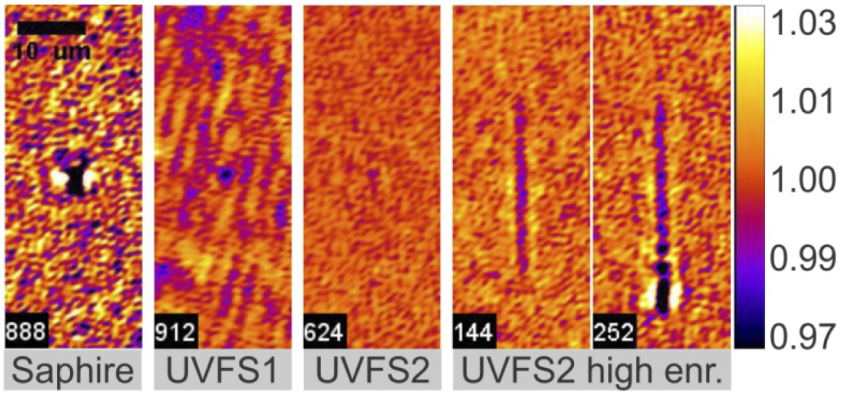

Fig. 4. Normalised transmission photos of initial modifications 2 seconds after exposure: sapphire (0.85 μJ), UVFS1(0.79 μJ), UVFS2(0.42 μJ) at low energy and UVFS2(0.5 μJ) at high energy.

3.1. Fused quartz

Figure 5 displays the relationship between the pulse energy and the number of pulses required to observe the modification of fused quartz samples. The damage is deterministic in nature as damage probability sharply rises from zero to one with increase in incident energy for 2500 on 1 damage test. The *post mortem* photos of the affected volume were normalised against the reference photo to increase the sensitivity of the approach. This way changes in transmission as small as 1% could be identified as modification. This limit was imposed by the background transmission noise with a standard deviation of 0.3 %. Interestingly, while both damage and

OPTICS CONTINUUM

increase in refractive index modification can be observed in UVFS2 sample, no refractive index change prior to damage can be seen for UVFS1. A clear trend in both samples is that with increase in energy the dose necessary for damage becomes more strictly defined.

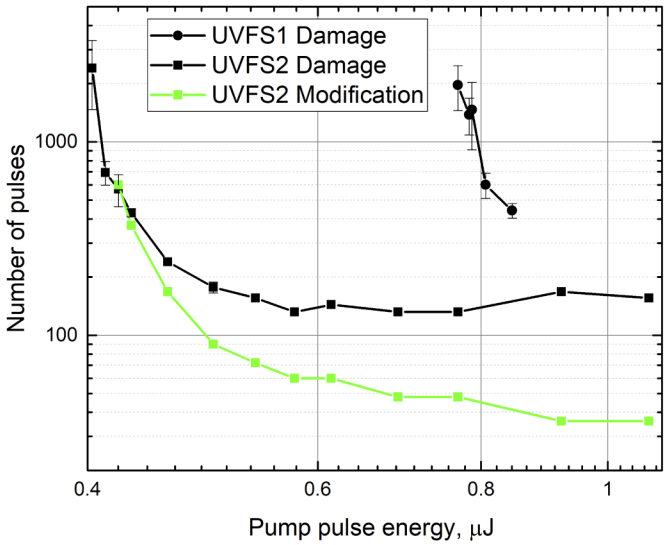

Fig. 5. Pulses required to induce apparent change (either modification or damage) versus applied laser pulse energy. No damage was observed at 2500 pulses with 0.749 μJ(UVFS1) and 0.403 μJ(UVFS2)

In case of UVFS1 sample, the dose necessary for damage seems to be less deterministic similar to UVFS2 at low energies. The variance in the number of pulses required to produce damage increases as the pump energy decreases. The damage initially appears as a negative phase shift corresponding to higher refractive index with value close to the noise limit. In transmission mode, shown in Fig. 4, it looks like a blur with the dimensions smaller than the diffraction limit of the current setup. As the pulses accumulate, the region with the increased refractive index grows and slowly translates in the direction opposite to the propagation of the beam. The negative phase shift becomes positive with further exposure. According to the data presented in [24], the pumping conditions used in this work are in range for void formation, which could explain why the final damage is registered as a decrease in the refractive index. Looking at the formation and the morphology of these damage points it can be seen that the origin overlaps the region of electron plasma generation. However, the exact position within this volume is not strictly defined. The position of the origin changes when the sample is translated. The coordinate along the axis of propagation across the observed zone of excitation (25 μm in length at 0.82 μJ) differ by up to 10 μm. This indicates that the damage origin could depend on the local quality of the material or the presence of intrinsic defects and may not coincide with the peak excitation.

The damage morphology, if compared at the same energy levels, seems to differ in between the two UVFS samples. The UVFS2 sample exhibits a more deterministic modification mechanism - slowly changing properties throughout the excited region and at significantly lower input energy values. In case of UVFS2, the modification of the material starts as a soft localised reduction in refractive index supported by phase shift data and normalised transmission integral equating to unity. After sufficient number of excitation events, this structure collapses into several damage points. However, the collapse is only observed at higher excitation pulse energies (E>0.5μJ). In contrast, below the interaction bellow 0.5μJ the nondeterministic mechanism starts dominating

OPTICS CONTINUUM

and the optical damage appears before significant refractive index change is observed. In this case, the damage formation is similar to that of UVFS1 sample.

According to the spectra shown in Fig. 2 the absorption in the UV-visible region is nearly identical. The main difference between the samples is in the peaks corresponding to the OH-groups [25]. It is significantly more pronounced in UVFS2 sample, with 1.5 increase in intensity. It is interesting to note that typically, OH- groups are introduced in quartz based fibers to improve their parameters in the UV range (reduced minimum absorption wavelength) [26]. On one hand, this should reduce the probability of multiphoton ionization. On the other hand, OH- ions are known to be precursors to the non bridging oxygen hole center (NBOHC, ≡Si-O•) [27], which could be an important factor in our experiments. As is shown that UVFS2, the sample exhibiting higher OH- concentration, produces significantly more free electron plasma and STE than UVFS1 at the same incident energy.

Figure 6 depicts how the phase shift due to free-electron plasma changes as a function of the number of applied laser pulses. The density of the free electron plasma can be evaluated using Drude model and extrapolating the two dimensional phase shift map to three dimensional phase shift distribution as described in Ref. [28]. However, not to underestimate the density, the relaxation of free electron plasma must also be considered. The pump pulse duration is 360 fs and is longer than the characteristic time of free-electron plasma relaxation in UVFS, which is estimated at 170 fs [23]. The time delay of the observation is approximately 300 fs from moment of maximum intensity, and cannot be reduced any further due to overlap between optical Kerr effect and free electron plasma signals. Assuming the worst case scenario, that the plasma is not regenerated by the trailing part of the pulse, the peak free electron density could be at most 4 times higher than the one registered using TRDH. Taking this factor into account the maximum estimated free electron density value right before the initiation of optical damage would be $6 \cdot 10^{19} cm^{-3}$. This estimated worst case concentration of free electrons is still well bellow critical density which is believed to be in the vicinity of $1.0 \cdot 10^{21} cm^{-3}$ - a value commonly used as a criterion for optical damage [19].

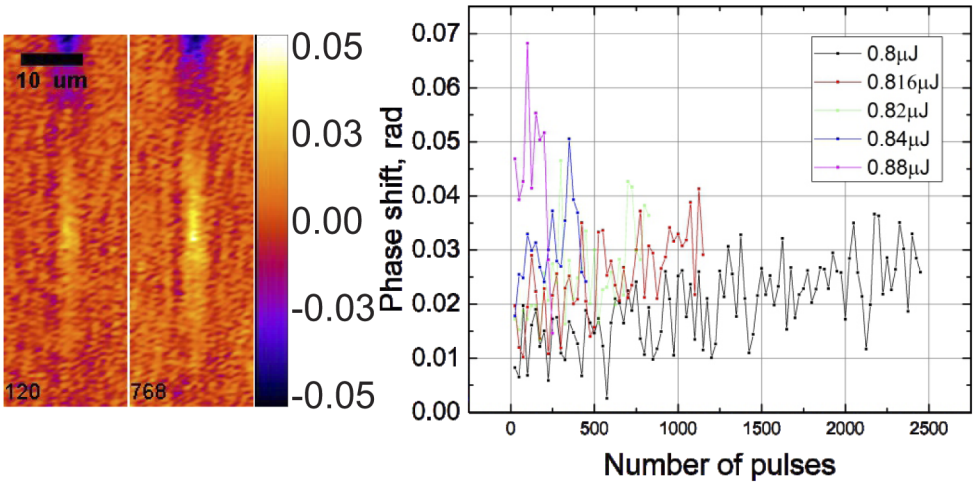

Fig. 6. On the left - phase shift map of free electron plasma in radians induced by 0.783 μJ pulse at 300 fs delay. On the right - graph of free electron plasma signal a function on the number of pulses prior to catastrophic damage in UVFS1.

At low energies, UVFS2 exhibits free electron plasma induced response similar to UVFS1. However, with increase in pump energy or number of pulses, the signal of electron plasma quickly begins to overlap with the signal of self-trapped excitons. This prevents us from correctly

OPTICS CONTINUUM

evaluating the electron density before optical damage for UVFS2 sample. It is unclear whether the accumulation effects change the dynamics of electron relaxation or this change is caused by the increase in value of self-trapped exciton density. However, this did not impact the measurements of STE signal. Figure 7 shows the dependence of phase shift due to self-trapped excitons in UVFS1 and UVFS2 as a function of the number of incident pulses at different excitation energies. The exciton signal seems to follow the free electron plasma signal at low energies, growing with increasing number of pulses. The spatial distribution of excitons seems to be more narrow than that of electron plasma. This indicates that there is a nonlinear relationship between the free electron density and self-trapped excitons. It can also be seen that in UVFS2 for higher incident energies the peak phase shift seems to saturate right before the damage occurs. By comparing the response at different incident energy pulses it can be observed that the maximum density of self-trapped exciton is not reached. Higher energy pulses result in larger density values. Furthermore, the analysis of the phase shift maps at different number of pulses shows that the distribution of excitons elongates in the direction opposite to pump propagation. This means that the absorbing volume grows and shifts closer to the surface of the sample and less energy reaches the deeper sections. In other words, multiple pulses enhance intensity clamping by increasing absorption in larger volume. Intensity clamping could be responsible for the saturation of exciton signal. In turn this implies saturation of free electron plasma density, assuming that the relation between electron plasma and self-trapped exciton density is analogous to that observed in UVFS1. This indicates that the formation of damage is not directly connected to free electron plasma density but perhaps is more closely related to the phenomena observed when using nanosecond pulses. Nonlinear absorption can create high energy electron plasma that has a similar ionizing effect as high energy photons. This could lead to generation of colour centers. Color center-induced stress could exceeded the mechanical strength of the material leading to optical damage. This could explain the formation of the observed refractive index modification and subsequent fragmentation.

3.2. Sapphire

The defining trait of nondeterministic damage is that step function cannot be used to approximate the damage probability in energy space and that smooth increase in probability is observed. The probability of optical damage in this experiment was calculated by taking the total number of sites and using it to divide the number of damage event of same energy. It can be seen in Fig. 8, how with increase in energy the probability of damage increases and the average dose needed to observe the optical damage decreases. This data supports that in sapphire, the damage is strongly nondeterministic and shows a stark contrast to the case of UVFS where the number of pulses required to trigger damage shows a clear asymptotic growth with decrease in energy. The probabilistic nature is evident even at the highest investigated energies there are positions where no damage was observed even with maximum investigated dose. Furthermore, the position of the damage origin also changes up to 15 μm along the length of the excited zone and does not necessary coincide with the peak electron signal. This indicates defect driven damage as a main factor limiting lifetime of sapphire. The initiation of the damage is similar to that observed in fused quartz at low energies - it starts as point source and then grows in the opposite direction to the propagation of the pulse. Judging by the significant phase distortion and shape it seems like the mechanism of expansion is different, data is pointing towards cracking. This can be related to the higher hardness and brittleness of sapphire as opposed to glass. Alternatively, it may be caused by the crystalline structure of sapphire, as opposed to amorphous fused silica. A systematic study involving more materials and including crystalline quartz could help to answer this question.

The typical phase shift images recorded in sapphire are shown in Fig. 9. The data shows no measurable difference between the response of the initial excitation and the one before the

OPTICS CONTINUUM

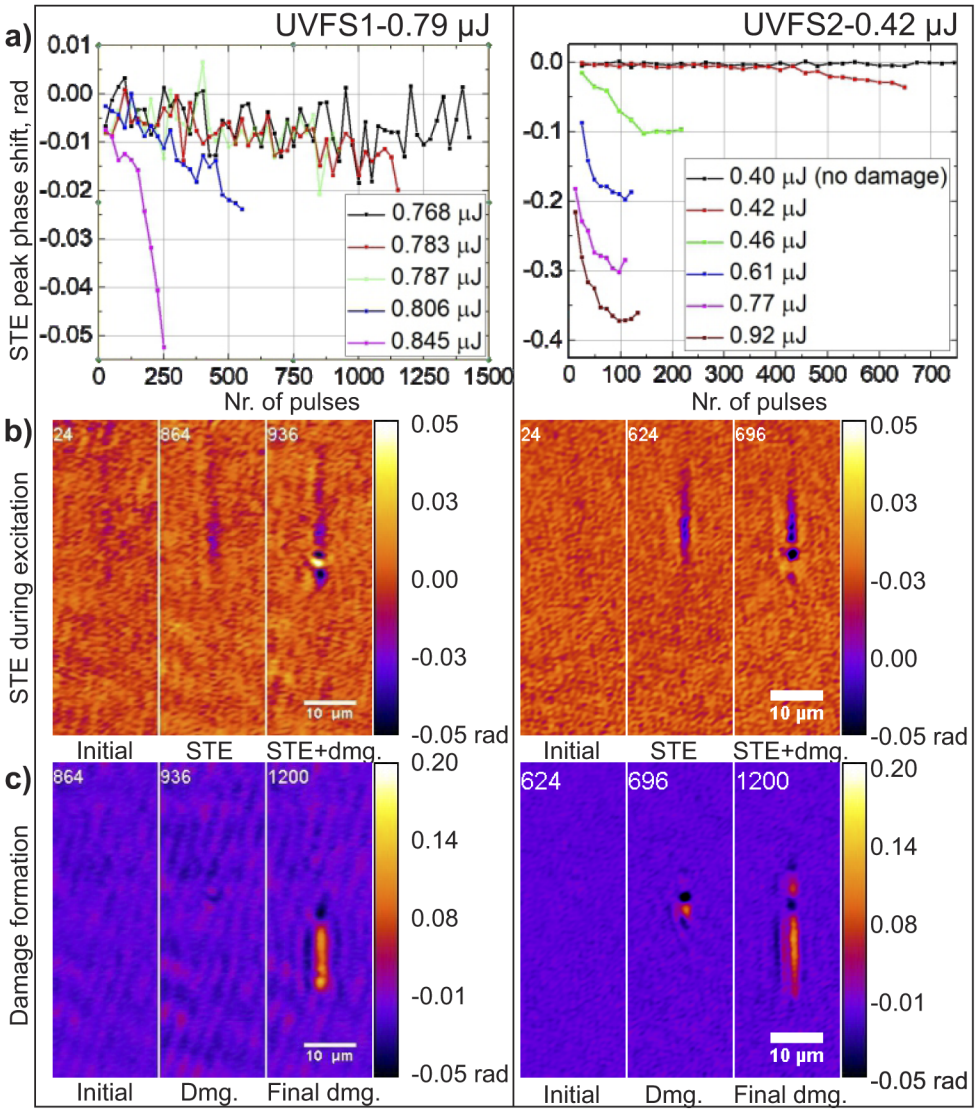

Fig. 7. a) STE signal vs the number of pulses prior to optical catastrophic damage in quartz samples, measured at the position of damage initiation. b) Phase shift map illustrating STE distribution at 1.1 ps delay at various number of pulses. c) Changes in permanent optical modification with further exposure observed 2 s after light matter interaction.

OPTICS CONTINUUM

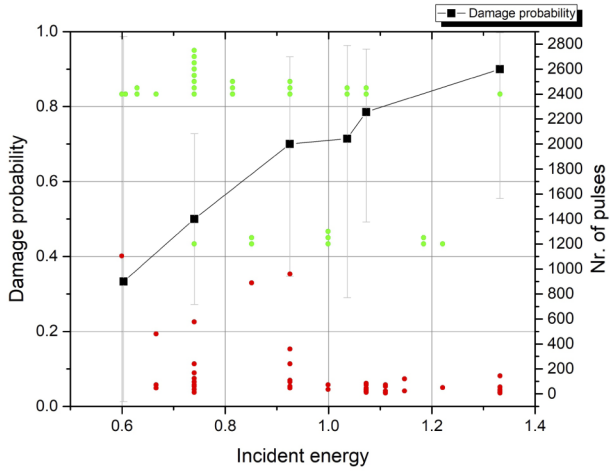

Fig. 8. The damage events (red dots), no observable damage (green dots) and damage probability for 1200-on-1 test in sapphire sample as a function of incident energy.

catastrophic damage. No spikes that would indicated local increase in electron plasma density were observed. The peak density increases slightly with higher incident pulse energy, likely due to intensity clamping effect. This is supported by growth of observed plasma volume: excited zone is 1.5 longer at 1.33 than at $0.6\mu J$. The estimated peak density of electron plasma prior to optical damage formation varies in the range: $1.3 - 2.4 \cdot 10^{20} cm^{-3}$ depending on pump intensity. The lack of any feedback loop can be the explanation for the high variance in the dose necessary to observe damage. With fused quartz the maximum number of pulses that the material can survive is limited by the increase in absorbed energy. Meanwhile, in sapphire the lack of such a mechanism means the material response does not change and therefore it can survive numerous exposures unless there is intrinsic weakness in the exposed volume. This is the main difference between the materials - the strong position dependence on damage probability, which can be explained by the defect densities between the two. This may arise from the natural differences between amorphous material and crystal lattice structure. Damage morphology together with the nondeterministic nature of the damage at low energies in all the samples suggest that defects play a significant role in multi-pulse optical damage even with ultrashort pulses. A larger study of optical fatigue involving a number crystalline and amorphous materials could provide additional insight in the role of material homogeneity (crystalline versus amorphous phase) in the pheonomena of optical fatigue and damage.

OPTICS CONTINUUM

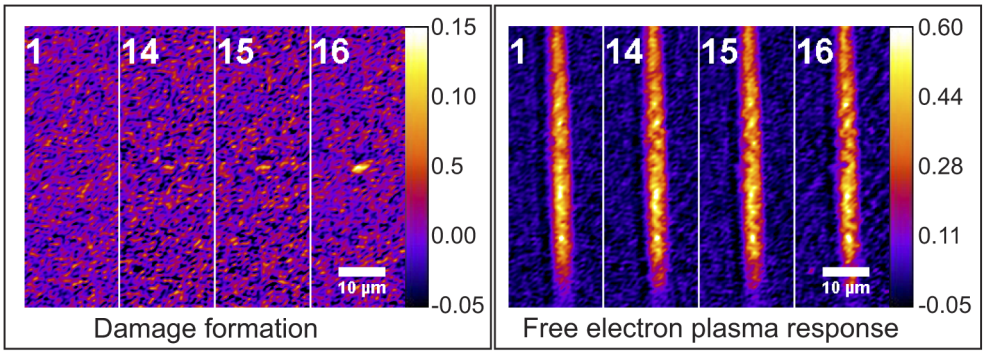

Fig. 9. Left - optical damage formation in sapphire(1.33 μJ). Right - preceding free electron plasma distribution including optical damage caused distortion in the center at 2 ps delay.

4. Conclusions

Distinct morphologies of initial damage and the differences in material response reinforces the existence of several mechanisms behind multi-pulse damage formation in bulk media in ultrashort pulse range. Experiments in bulk fused quartz confirm charge carriers and self-trapped excitons both play a role in multi-pulse damage formation. The increase in the signal with repeated exposures illustrates the increase in deposited energy and contributes to the more deterministic nature of optical damage for higher energies. Importantly, critical electron plasma density can not be used as a criterion to determine optical multi-pulse damage in bulk media: the formation of damage is observed at plasma densities orders of magnitude below critical value. The variance in number of pulses necessary to trigger damage increases in all the investigated samples, as pulse energies decrease. In sapphire, damage probability depends mostly on the irradiated sample spot. This may be due to lower density of defects in the crystalline lattice. All of this suggest defect driven damage despite the ultrafast regime.

Funding. European Regional Development Fund, "Research Projects Implemented by World-Class Researcher Groups" (01.2.2-LMT-K-718 (-01-0014)).

Disclosures. The authors declare no conflicts of interest.

Data availability. Data underlying the results presented in this paper are not publicly available at this time but may be obtained from the authors upon reasonable request.

References

1. X. Ling, "Nanosecond multi-pulse damage investigation of optical coatings in atmosphere and vacuum environments," Appl. Surf. Sci. **257**(13), 5601–5604 (2011).
2. P. Rajeev, M. Gertsvolf, E. Simova, C. Hnatovsky, R. Taylor, V. Bhardwaj, D. Rayner, and P. Corkum, "Memory in nonlinear ionization of transparent solids," Phys. Rev. Lett. **97**(25), 253001 (2006).
3. A. Chmel and S. Eronko, "Optical strength of glasses implanted with argon ions," Glass technology **39**, 32–34 (1998).
4. S. C. Jones, P. Braunlich, R. T. Casper, X.-A. Shen, and P. Kelly, "Recent Progress On Laser-Induced Modifications And Intrinsic Bulk Damage Of Wide-Gap Optical Materials," Opt. Eng. **28**(10), 1039–1068 (1989).
5. P. Braunlich, S. C. Jones, S. Xiao-An, R. T. Casper, and P. Kelly, "Laser-induced modifications and the mechanism of intrinsic damage in wide gap optical materials," Nucl. Instruments Methods Phys. Res. Sect. B: Beam Interactions with Mater. Atoms **46**(1-4), 224–230 (1990).
6. B. Gorshkov, Y. Danileiko, V. Nikolaev, and A. Sidorin, "Effect of multiple irradiation upon exposure of optical material to laser radiation," Kvantovaya Elektron **10**, 640–643 (1983).
7. L. Glebov, V. Dokuchaev, O. Efimov, N. Nikonorov, and G. Petrovskii, "Role of radiation-induced color centers in the development of optical breakdown in silicate glasses," Izv. Akad. Nauk SSSR, Ser. Fiz **49**, 1179–1181 (1985).
8. D. Von der Linde and H. Schüler, "Breakdown threshold and plasma formation in femtosecond laser–solid interaction," J. Opt. Soc. Am. B **13**(1), 216–222 (1996).
9. A. Chmel, "Fatigue laser-induced damage in transparent materials," Mater. Sci. Eng., B **49**(3), 175–190 (1997).
10. J. Krüger, M. Lenzner, S. Martin, M. Lenner, C. Spielmann, A. Fiedler, and W. Kautek, "Single-and multi-pulse femtosecond laser ablation of optical filter materials," Appl. Surf. Sci. **208-209**, 233–237 (2003).

OPTICS CONTINUUM

11. M. Mero, B. R. Clapp, J. C. Jasapara, W. G. Rudolph, D. Ristau, K. Starke, J. Krüger, S. Martin, and W. Kautek, "On the damage behavior of dielectric films when illuminated with multiple femtosecond laser pulses," Opt. Eng. **44**(5), 051107 (2005).
12. L. Yuan, Y. Zhao, H. He, J. Shao, and Z. Fan, "Single-pulse and multi-pulse femtosecond laser damage of optical single films," High Power Laser and Particle Beams **18**, 595–598 (2006).
13. L. A. Emmert, M. Mero, and W. Rudolph, "Modeling the effect of native and laser-induced states on the dielectric breakdown of wide band gap optical materials by multiple subpicosecond laser pulses," J. Appl. Phys. **108**(4), 043523 (2010).
14. L. Smalakys, E. Drobužaitė, B. Momgaudis, R. Grigutis, and A. Melninkaitis, "Quantitative investigation of laser-induced damage fatigue in hfo2 and zro2 single layer coatings," Opt. Express **28**(17), 25335–25345 (2020).
15. A. Rudenko, J.-P. Colombier, T. E. Itina, and R. Stoian, "Genesis of nanogratings in silica bulk via multipulse interplay of ultrafast photo-excitation and hydrodynamics," Adv. Opt. Mater. **9**(20), 2100973 (2021).
16. L. B. Glebov, O. M. Efimov, G. T. Petrovskiĭ, and P. Rogovtsev, "Influence of the mode composition of laser radiation on the optical breakdown of silicate glasses," Sov. J. Quantum Electron. **14**(2), 226–229 (1984).
17. L. B. Glebov, O. M. Efimov, N. V. Nikonorov, and G. T. Petrovskiĭ, "Optical breakdown of the surface of k8 glass modified by low-temperature ion exchange," Sov. J. Quantum Electron. **15**(10), 1410–1412 (1985).
18. O. Efimov, S. Juodkazis, and H. Misawa, "Intrinsic single-and multiple-pulse laser-induced damage in silicate glasses in the femtosecond-to-nanosecond region," Phys. Rev. A **69**(4), 042903 (2004).
19. B. Stuart, M. Feit, A. Rubenchik, B. Shore, and M. Perry, "Laser-induced damage in dielectrics with nanosecond to subpicosecond pulses," Phys. Rev. Lett. **74**(12), 2248–2251 (1995).
20. Z. Sun, M. Lenzner, and W. Rudolph, "Generic incubation law for laser damage and ablation thresholds," J. Appl. Phys. **117**(7), 073102 (2015).
21. T. Balciunas, A. Melninkaitis, G. Tamosauskas, and V. Sirutkaitis, "Time-resolved off-axis digital holography for characterization of ultrafast phenomena in water," Opt. Lett. **33**(1), 58–60 (2008).
22. U. Schnars, C. Falldorf, J. Watson, and W. Jüptner, "Digital holography," in *Digital Holography and Wavefront Sensing*, (Springer, 2015), pp. 39–68.
23. Q. Sun, H. Jiang, Y. Liu, Z. Wu, H. Yang, and Q. Gong, "Measurement of the collision time of dense electronic plasma induced by a femtosecond laser in fused silica," Opt. Lett. **30**(3), 320–322 (2005).
24. B. Poumellec, M. Lancry, A. Chahid-Erraji, and P. G. Kazansky, "Modification thresholds in femtosecond laser processing of pure silica: review of dependencies on laser parameters," Opt. Mater. Express **1**(4), 766–782 (2011).
25. B. Sloots, "Measuring the low oh content in quartz glass," Vib. Spectrosc. **48**(1), 158–161 (2008).
26. C. Campanella, V. De Michele, A. Morana, G. Mélin, T. Robin, E. Marin, Y. Ouerdane, A. Boukenter, and S. Girard, "Radiation effects on pure-silica multimode optical fibers in the visible and near-infrared domains: Influence of oh groups," Appl. Sci. **11**(7), 2991 (2021).
27. L. Skuja, K. Kajihara, M. Hirano, and H. Hosono, "Visible to vacuum-uv range optical absorption of oxygen dangling bonds in amorphous sio_2," Phys. Rev. B **84**(20), 205206 (2011).
28. B. Momgaudis, V. Kudriasov, M. Vengris, and A. Melninkaitis, "Quantitative assessment of nonlinearly absorbed energy in fused silica via time-resolved digital holography," Opt. Express **27**(5), 7699–7711 (2019).